Quantum chaos of Ar_3: Statistics of eigenvalues

David M. Leitner and R. Stephen Berry
Department of Chemistry and the James Franck Institute, The University of Chicago, Chicago, Illinois 60637

Robert M. Whitnell
Department of Chemistry, B-039, University of California at San Diego, La Jolla, California 92093

(Received 14 April 1989; accepted 18 May 1989)

The successive diagonalization–truncation method is applied to the calculation of the vibrational eigenvalues of the Ar trimer bound by pairwise Lennard-Jones potentials. The statistics of the eigenvalues reveal strongly chaotic behavior of the cluster, consistent with the classical dynamics studies. Moreover, the zero-point energy is higher than the highest energy at which regular dynamics were found classically, indicating that for all energies physically accessible to the cluster, the dynamics are chaotic.

I. INTRODUCTION

The classical dynamics of a rotationless Ar_3 cluster bound by pairwise Lennard-Jones potentials was recently investigated.[1,2] The study explored a wide range of energies, from the low temperature, normal mode region to that near dissociation of the trimer, to probe how the ergodicity and chaos of the cluster vary with the energy. Although Ar_3 has relatively few degrees of freedom, it does embody some of the characteristics of larger clusters. At a critical energy, Ar_3 undergoes a change which might be called a phase change, and the distribution of kinetic energies for a range above that critical energy is bimodal. Classical Ar_3 also has some of the characteristics of a triatomic molecule, with a range of energy, though relatively narrow, where the dynamics are largely regular (or quasiperiodic) and characterized by nearly separable normal modes; then, at higher energies a transition to a region of increasingly chaotic behavior occurs.

The classical dynamics can be summarized as follows. The degree of ergodicity, quantified by the correlation dimension of the trajectory in the phase space, appears to be strongly correlated with the degree of chaos (characterized by K entropy) of the trimer, though such a correlation is not obvious *a priori*. There are three major ranges of energy within each of which a distinct type of dynamics is found. At very low energies, the behavior is dominated by nearly separable normal modes, with some mode–mode coupling apparent in the power spectrum of the velocity autocorrelation function, and a small but nonzero K entropy. The trajectory is restricted largely to a three-dimensional torus, although it wanders occasionally into a larger subspace of the phase space. In the next range of energy the dynamics is described by a steadily increasing K entropy that persists until the critical energy at which the "phase change" takes place. Above this critical energy, saddle regions in the configuration space, corresponding to linear Ar_3, are energetically accessible to the cluster. There, the K entropy and fractal dimension increase very slowly with energy. Much larger, two-dimensional clusters that undergo phase changes have been found to display similar behavior.[3]

The real cluster is, of course, quantum mechanical. Particularly at the lowest energies, one might expect quantum mechanics to make predictions different from its classical counterpart. Most quantum investigations of systems that are classically chaotic make use of the statistics of the distribution of the eigenvalues. Two statistical measures, which have been applied to a variety of systems, yield trends that are identifiable with the extent of chaos in the corresponding classical systems. These measures are the probability distribution of the nearest-neighbor level spacings, and the Δ_3 function, a measure of the fluctuations of the levels about a smoothed integrated density of states over a range of energy. Both approaches reveal the same trend: as the classical system becomes more chaotic, the statistics of the eigenvalue distributions and the Δ_3 function change from Poissonian to statistics that strongly resemble the Wigner eigenvalue statistics of a Gaussian orthogonal ensemble (GOE).[4]

In many cases, statistics of the vibrational levels of molecules[5] and electronic levels of atoms[6] are neither purely Poisson or Wigner, but something intermediate. Such statistics are found in making transitions from regular, quasiperiodic to chaotic behavior. It has been suggested that this appearance of intermediate behavior arises from the superposition of spectra due to levels associated with regular and chaotic regions in the phase space of the classical system.[7] At present, we have only empirical functions to describe an intermediate distribution. One, due to Brody,[8] which has been used by nuclear physicists for some time, varies smoothly between Poisson and Wigner distributions with the adjustment of a single parameter.

We have calculated the vibrational eigenvalues of Ar_3 using the successive diagonalization–truncation method[9(a)] and a three-dimensional discrete variable representation (DVR).[9(b),9(c)] The method was recently successfully applied to a trimer of the same symmetry, H_3^+.[9(c)] The probability distribution of the nearest neighbor level spacings and the Δ_3 function permit a direct comparison with the classical analysis. Below, we summarize the classical results, then discuss the method for the quantum mechanical calculations and statistics. Finally, we compare the classical and quantum results.

II. CLASSICAL Ar_3

Complete results of the classical dynamics study can be found in Refs. 1 and 2. Here, we review only the aspects relevant for comparison with the quantum results. The molecular dynamics simulations for Ar_3 were produced by solv-

 0021-9606/89/183470-07$02.10

ing the equations of motion for the Hamiltonian

$$H=\sum_{i=1}^{3}\frac{\mathbf{p}_i^2}{2m}+4\epsilon\sum_{i<j}^{3}\left[\left(\frac{\sigma}{\mathbf{r}_{ij}}\right)^{12}-\left(\frac{\sigma}{\mathbf{r}_{ij}}\right)^{6}\right]. \quad (1)$$

We use $\sigma=3.4$ Å and $\epsilon=1.67(10^{-14})$ erg. The potential has a well depth of 252 cm^{-1}. The cluster had no angular momentum and was limited, to the extent allowed by numerical roundoff error, to vibrational motion. From coordinates and momenta calculated by the simulations, the power spectra, Liapunov spectra, and fractal dimension of the trajectory in the phase space were calculated.

The molecular dynamics simulations were done over a wide range of energies, from 2% up to about 60% of the well depth. Simulations at slightly higher energies exhibit evaporation too rapid to allow study of the bound trimer. The effective temperatures, proportional to the mean kinetic energy over the length of the run, range from 2 to 41 K. At the low temperatures, between 2 and 10 K, the dynamics are regular, with some mode–mode coupling, indicated by the overtones in the power spectrum and a small but nonzero K entropy. The fractal dimension rises slowly over this range, indicating an increasing exploration of the phase space off the three-dimensional torus, the region of the phase space to which the integrable system is confined.

The next range of temperatures, above 10 to about 28 K, is characterized by a rapidly changing power spectrum whose peaks broaden with increasing temperature. Concurrently, the K entropy and correlation dimension, hence the quantitative levels of chaos and ergodicity, increase monotonically. The highest energy of this region is about two-thirds of the dissociation energy and corresponds to the saddle energy, below which each atom is confined to the potential well. It is noteworthy that at 28 K, the K entropy and dimensionality of the cluster have the highest values we found.

Just above the energy of 76 cm^{-1}, corresponding to 28 K, Ar_3 exhibits a change which, in several ways, resembles a phase change. The power spectra for all temperatures above 28 K exhibit nonzero intensities at zero frequency, indicating diffusive motion within the cluster. Such "diffusion" is really motion of the atoms over the saddle of the linear configuration. Both the fractal dimension and the K entropy drop above the phase change, at 30 K, then rise again slowly with increasing energy. Moreover, locally, the Liapunov spectrum and the fractal dimensions exhibit two kinds of behavior. The configuration space can be divided into two dynamically distinct regions, the saddle regions and the potential well. One can then break the trajectories into pieces lying in the dynamically distinct regions and calculate the Liapunov spectra and dimensions for the two regions separately. This procedure shows that motion over the saddle is relatively less chaotic and less ergodic than motion in the well. That is, the K entropy and fractal dimension are significantly lower in the saddle region than in the well. Moreover, the K entropy and fractal dimension rise only very slowly with energy for trajectory segments above the saddle. The drops in overall K entropy and dimension, averages over the whole trajectory, are explained by the low kinetic energy, long residencies, and "streaming" trajectories, that is by the regular motion, in the saddle region. By 149 cm^{-1}, or 41 K, the regions become indistinguishable, and the K entropy is constant with energy, or rises very slowly.

III. QUANTUM Ar_3

To calculate the vibrational spectrum of Ar_3, we employed the method used for the calculation of the H_3^+ spectrum. Whitnell and Light found the successive truncation–diagonalization technique in conjunction with the three-dimensional DVR to be very efficient for computing a large number of H_3^+ levels with angular momentum $J=0$.[9(c)] Because H_3^+ and Ar_3 have the same symmetry, D_{3h}, the methods used for H_3^+ can be tried for determining the eigenvalues of the larger system. This application must take into account both the larger mass and the weaker forces present in the Ar_3 system. Such a calculation, besides enabling exploration of the relationship between the quantum eigenstates and the classical chaos, also gives a good test of the robustness of the method for very different systems.

The successive truncation method, Pack's hyperspherical coordinate system, and the symmetry-adapted basis sets are all discussed in the recent articles.[9] The only modifications we required were changes in the potential in the Hamiltonian, here pairwise Lennard-Jones, in the masses of the atoms, and in various truncation parameters, which will be identified in the Results section.

We have performed two different statistical analyses of the eigenvalues corresponding to each of the irreducible representations A_1', A_2', and E', all symmetry allowed if we treat the Ar atoms as distinguishable. Each analysis reveals the degree of quantum chaos of the cluster for specific ranges of energies. Both approaches require calculating a new spectrum from the vibrational spectrum so that the density of states is the same over all regions of the spectrum. To calculate a new set of levels $\{\tilde{E}_1,\tilde{E}_2,...,\tilde{E}_n\}$ from the vibrational spectrum $\{E_1,E_2,...,E_n\}$, one needs to first unfold the spectrum, dividing all the level spacings by their local average,[5]

$$\tilde{E}_{i+1}=\tilde{E}_i+(2k+1)\frac{E_{i+1}-E_i}{E_{j_2+1}-E_{j_1}},$$
$$j_1=i-k\ \ (i-k>0),\quad j_2=i+k\ \ (i+k<n). \quad (2)$$

In practice, we use $k=3$, so that the average is over seven levels. Our results are not very sensitive to this number, since for most of the levels, the density of states changes slowly.

The first method is to calculate the probability distribution of the nearest-neighbor level spacings $P(s)$ of the unfolded spectrum. The distribution corresponds to the dynamics of the classical system. For systems in which the classical dynamics is regular, the distribution in the semiclassical limit has been proven to be the Poissonian,[10]

$$P(s)=\frac{1}{D}\exp\left[\frac{-s}{D}\right], \quad (3)$$

where s is the spacing of the unfolded spectrum and D is the mean level spacing, here always 1 because of the local normalization. Chaotic dynamical systems have distributions with a Wigner form

$$P(s) = \frac{\pi s}{2D^2} \exp\left[\frac{-\pi s^2}{4D^2}\right]. \quad (4)$$

Several functions have been defined to describe distributions intermediate to the Poisson and Wigner distributions.[7,8] One of them is the Brody distribution,

$$P(s) = A\left(\frac{s}{D}\right)^{\omega} \exp\left[-\alpha\left(\frac{s}{D}\right)^{1+\omega}\right], \quad (5)$$

where $A = (1+\omega)\alpha$ and $\alpha = \{\Gamma[(2+\omega)/(1+\omega)]\}^{1+\omega}$. Equation (3) is obtained if $\omega = 0$ and Eq. (4) if $\omega = 1$. We shall fit ω to the distribution to determine the function $P(s)$.

The statistic appropriate for the second method is the Δ_3 function proposed by Dyson and Mehta,[11]

$$\Delta_3(r) = \left\langle \min_{a,b} \frac{1}{L} \int_0^L [N(\tilde{E}) - a\tilde{E} - b]^2 d\tilde{E} \right\rangle. \quad (6)$$

Here, L is the total energy interval, $r = L/D$ is the mean number of energy levels, and $N(\tilde{E})$ is the number of levels with energy less than $\tilde{E}N(\tilde{E}) = \Sigma_i \Theta(\tilde{E} - \tilde{E}_i)$. While the distribution of nearest-neighbor spacings is a measure of the local fluctuations around each level, Δ_3 is a measure of the average fluctuations within a region of energy. The interpretation of Eq. (6) is that fitting a straight line through $N(\tilde{E})$, Δ_3 represents the integrated square displacement of the staircase from that line as a function of the size of the unfolded energy interval.

Equation (6) can be expressed in a form convenient for numerical computation,[12]

$$\Delta_3(r) = \left\langle \frac{-1}{L} \sum_{i=1}^{R} (2i-1)\tilde{E}_i + \frac{2R}{L} \sum_{i=1}^{R} \tilde{E}_i - \frac{4}{L^2}\left[\sum_{i=1}^{R} \tilde{E}_i\right]^2 - \frac{3}{L^4}\left[\sum_{i=1}^{R} \tilde{E}_i^2\right]^2 + \frac{6}{L^3}\left[\sum_{i=1}^{R} \tilde{E}_i^2\right]\cdot\left[\sum_{i=1}^{R} \tilde{E}_i\right] \right\rangle, \quad (7)$$

where r is the mean number of energy levels for a given range in energy L, and $\langle\ \rangle$ denotes an ensemble average. R is the actual number of levels in the same energy range of some region of the unfolded spectrum. To obtain Δ_3 for an r, one averages sequences of R levels throughout the length of the unfolded spectrum.

For a Poisson distribution, $\Delta_3 = r/15$. The relation in the chaotic limit, which is identical to that of Gaussian orthogonal ensembles (GOE) of random matrix theory,[11] is

$$\Delta_3(r) = \frac{1}{\pi^2}(\ln r - 0.0687). \quad (8)$$

For many systems, one finds functions intermediate between the Poisson and the GOE relations, indicating dynamics that are part regular and part chaotic.

IV. RESULTS AND DISCUSSION

Results of the 3D DVR calculation for the A_1', A_2', and E' representations are listed in Tables I, II, and III, respectively. For each representation, the tabulated eigenvalues have converged to 1 cm^{-1}. It is significant that the distributions for each representation converge much faster than the eigenvalues; namely, the histograms of the energy level separations quickly attain almost constant shape as the size of the calculation increases. We checked this quantitatively by computing the Brody parameter ω for distributions obtained from matrices of increasing basis size.

TABLE I. Eigenvalues of Ar_3; A_1' representation.

State	Energy (cm^{-1})	State	Energy
1	37.35	45	147.20
2	63.07	46	147.52
3	73.28	47	148.71
4	84.15	48	149.61
5	88.42	49	149.73
6	94.04	50	149.91
7	97.33	51	150.79
8	101.45	52	151.81
9	103.68	53	152.09
10	104.97	54	152.43
11	106.61	55	153.55
12	107.78	56	154.61
13	108.98	57	154.83
14	111.45	58	155.30
15	113.01	59	156.32
16	114.52	60	156.85
17	117.02	61	156.95
18	118.93	62	157.76
19	121.78	63	157.97
20	123.02	64	159.16
21	123.47	65	159.40
22	124.49	66	159.74
23	124.96	67	159.88
24	126.60	68	160.79
25	127.11	69	161.37
26	128.04	70	161.60
27	129.71	71	162.13
28	131.87	72	162.63
29	132.00	73	162.93
30	132.87	74	163.47
31	134.82	75	163.85
32	136.32	76	164.75
33	137.43	77	165.10
34	138.03	78	165.14
35	138.08	79	165.31
36	138.85	80	166.16
37	140.14	81	166.42
38	140.83	82	166.91
39	142.03	83	167.29
40	142.85	84	167.67
41	143.50	85	167.99
42	144.18	86	168.41
43	144.82	87	168.57
44	145.82	88	169.19

The cutoff energy was 0.022 eV, and the permitted values of the hyperspherical dilation coordinate ρ were in the interval 7.5 to 16.0 a.u. For the A_1' representation, 18 DVR points were used in each of the hyperspherical coordinates θ, ρ, and χ. The dimension of the matrix after truncation was 1186. For the A_2' representation, with 16 DVR points, a matrix dimension of 844 after truncation was used. Fifteen DVR points were used in each coordinate of E', which produced a matrix dimension of 1128 after truncation. While the convergence of the eigenvalues in these calculations is not as good as that for H_3^+, these results indicate that the lowest energy vibrational eigenstates of van der Waals sys-

TABLE II. Eigenvalues of Ar_3; A_2' representation.

State	Energy (cm^{-1})	State	Energy
1	91.27	46	168.40
2	106.51	47	169.78
3	116.09	48	170.32
4	121.41	49	170.75
5	124.31	50	170.84
6	128.09	51	171.83
7	130.80	52	172.21
8	132.49	53	172.58
9	134.02	54	172.83
10	135.71	55	173.11
11	137.63	56	173.75
12	139.86	57	174.13
13	141.79	58	174.78
14	142.14	59	174.93
15	143.62	60	175.97
16	144.61	61	176.11
17	144.89	62	176.97
18	145.73	63	177.09
19	147.59	64	177.57
20	148.42	65	178.16
21	150.42	66	178.64
22	151.59	67	179.15
23	152.71	68	179.38
24	153.56	69	179.79
25	154.12	70	179.85
26	154.92	71	180.42
27	155.64	72	181.06
28	156.50	73	181.61
29	157.27	74	181.84
30	158.25	75	181.98
31	159.39	76	182.18
32	159.69	77	182.65
33	160.68	78	182.81
34	160.99	79	183.49
35	161.77	80	183.71
36	163.05	81	183.80
37	163.53	82	184.72
38	164.50	83	185.37
39	165.08	84	185.47
40	165.31		
41	166.07		
42	166.17		
43	167.13		
44	167.59		
45	168.03		

TABLE III. Eigenvalues of Ar_3; A_2' representation.

State	Energy (cm^{-1})	State	Energy
1	51.38	45	134.74
2	56.37	46	136.13
3	72.52	47	136.59
4	73.52	48	137.06
5	77.44	49	137.72
6	85.30	50	138.45
7	91.41	51	139.79
8	92.91	52	140.24
9	94.19	53	140.42
10	97.13	54	140.74
11	97.29	55	141.37
12	100.92	56	141.88
13	104.66	57	141.96
14	105.15	58	142.36
15	107.71	59	142.80
16	108.54	60	143.21
17	109.74	61	143.55
18	110.49	62	144.10
19	111.45	63	144.41
20	112.63	64	145.22
21	113.53	65	145.60
22	114.98	66	145.98
23	115.99	67	146.39
24	119.30	68	147.14
25	120.19	69	147.53
26	121.36	70	147.59
27	121.72	71	148.17
28	121.76	72	148.94
29	123.67	73	149.08
30	123.93	74	149.17
31	124.54	75	150.34
32	125.75	76	150.61
33	126.87	77	151.07
34	127.65	78	151.53
35	127.95	79	151.66
36	128.24	80	152.10
37	128.75	81	152.23
38	130.04	82	152.63
39	131.38	83	152.77
40	131.91	84	153.32
41	132.25	85	153.72
42	132.41	86	154.12
43	133.38	87	154.20
44	133.72	88	154.60

tems can be determined quite accurately. The higher energy states are certainly not located to spectroscopic accuracy, but the convergence is sufficient to determine the distributions central to this work.

The very low energies probed classically are never accessed by the quantum system. The zero-point energy of 37 cm^{-1}, or 15% of the well depth of 252 cm^{-1}, is above the low-energy range in which classical motion is largely regular. Therefore, the real Ar_3 cluster has no such regular physical region; all its states lie in the classical chaotic range.

It is impossible to describe statistically the region of energy below the phase change because there are at most only six eigenvalues in any representation with energies below the saddle energy. We must therefore settle for a larger range of energies, where the density of states becomes high due to the large masses of the Ar atoms. For each symmetry, we have been able to use energies up to about 187 cm^{-1}.

Figures 1–3 present the normalized histograms of the distributions of nearest-neighbor level spacings for A_1', A_2', and E' representations, respectively. In each figure, the Poisson and Wigner functions have been superimposed to show how Wigner-like each distribution is. Although none of the distributions fit the limiting cases precisely, they all seem to resemble the Wigner function much more than the Poisson. To better quantify how close the distributions are to a Wigner distribution, we have calculated the parameter ω of Eq. (4), obtained by fitting our distribution to Eq. (4), and the moments of our distributions[13]; these are presented in Table IV. The values indicate that the distributions for the representations of Ar_3 are very close to Wigner distributions.

TABLE IV. Moments of the nearest-neighbor spacings distributions of the vibrational eigenvalues of Ar_3 and parameter ω of Eq. (6), obtained numerically by a nonlinear least-squares-fitting procedure, $\overline{S}$, $\overline{S}^2$, and $\overline{S}^3$ are the first, second, and third moments, respectively.

Distributions	$\overline{S}^2/(\overline{S})^2$	$\overline{S}^3/(\overline{S})^3$	ω
Poisson	2	6	0
Wigner	$4/\pi \approx 1.27$	$6/\pi \approx 1.91$	1
A_1'			
1 to 66	1.30	2.00	0.88
67 to 132	1.29	1.97	0.90
A_2'			
1 to 84	1.34	2.20	1.0
E'			
1 to 117	1.28	1.95	0.90
118 to 234	1.22	1.74	1.27

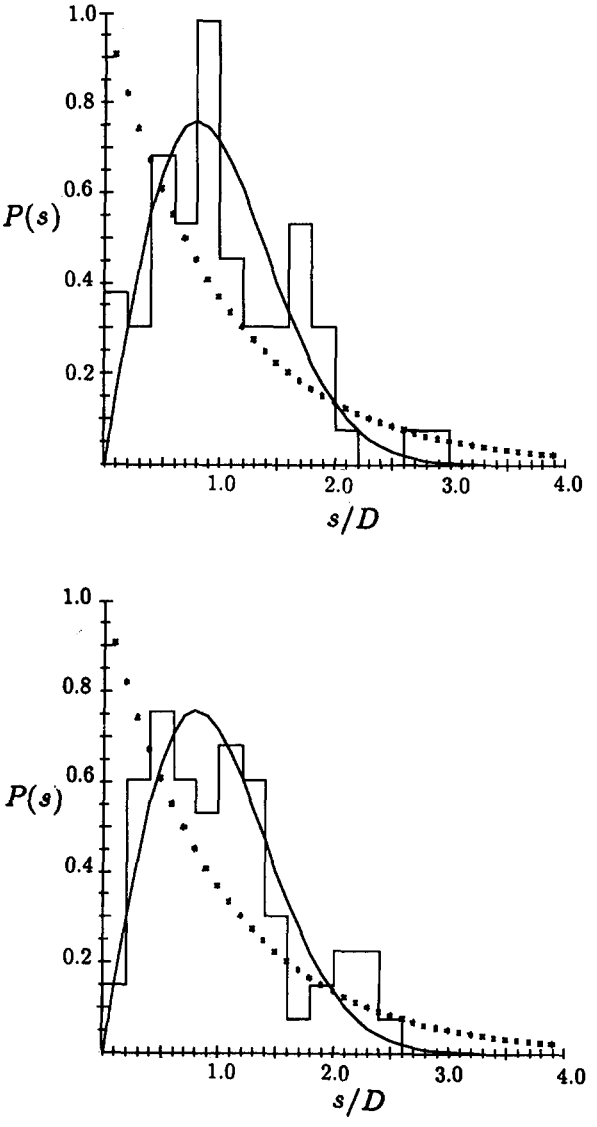

FIG. 1. The nearest-neighbor level spacings distribution for the A_1' representation. Superimposed are the Poisson [Eq. (3), plotted with *] and Wigner [Eq. (4), plotted with solid line] distributions. (a) is the first 66 levels, up to 159 cm^{-1}. (b) includes the next 66 levels, up to 180 cm^{-1}.

Deviations from the Wigner values could simply be the result of the statistics of only a limited number of levels.

The A_1' and E' representations have enough levels to allow calculating a sequence of distributions, found in Figs. 1(a) and 1(b), and 3(a) and 3(b). There is no substantial difference between the distributions formed by the first or the second set of levels for either of the representations. The classical study revealed that the degree of chaos is near its maximum at the saddle energy, falls, and then rises only very slowly with energy above the saddle energy. The very close resemblance to Wigner functions of each of the distributions is entirely consistent with the classical findings.

The Δ_3 statistic, plotted in Figs. 4–6, provides the same kind of evidence for strongly chaotic behavior as do the level spacing distributions. Again, the functions are intermediate, but resemble the Wigner function, plotted using Eq. (7), much more strongly than the Poisson function. The plot corresponding to the A_2' representation resembles the Wigner function most. Again, we plotted a sequence of levels for the A_1' and E' representations, Figs. 4(a) and 4(b) and 6(a) and 6(b), respectively. There is no indication that the system becomes more chaotic with increasing energy, the same conclusion we reached from the classical analysis and the distribution of spacings.

Because Ar is a spinless boson, only A_1' representation is needed for $J=0$. However, the other representations become important when rotation is included. Results of the statistical analyses suggest chaotic dynamics for all accessible levels of the A_1' representation. The probability function and Δ_3 function strongly resemble GOE statistics. The other representations, calculated to compare with the classical results, similarly demonstrate GOE statistics, so there is no difference between the quantum and classical predictions in this respect.

V. CONCLUSIONS

We have successfully applied the successive diagonalization–truncation method with the three-dimensional DVR to calculating the vibrational levels of Ar_3. Though most of the levels that we computed are not of the spectroscopic accuracy reached for H_3^+, the levels calculated for the larger Ar_3 system are converged enough to evaluate statistically, in order to determine the dynamical properties of the cluster. We expect that the technique may be directly applied to other trimers with D_{3h} symmetry, at least to evaluate some of their statistical properties. For rotationless states of bosons, only the basis in the A_1' representation needs to be solved. We computed the eigenvalues in the A_2' and the E' representations as well to treat the atoms as identical particles in the classical sense, to compare with the classical studies.

The nearest-neighbor level distributions, and their moments, as well as the Δ_3 function indicate for each representation that the cluster is chaotic for all accessible energies. These statistics closely resemble GOE statistics. Moreover, the statistics for successive ranges of energy are close to

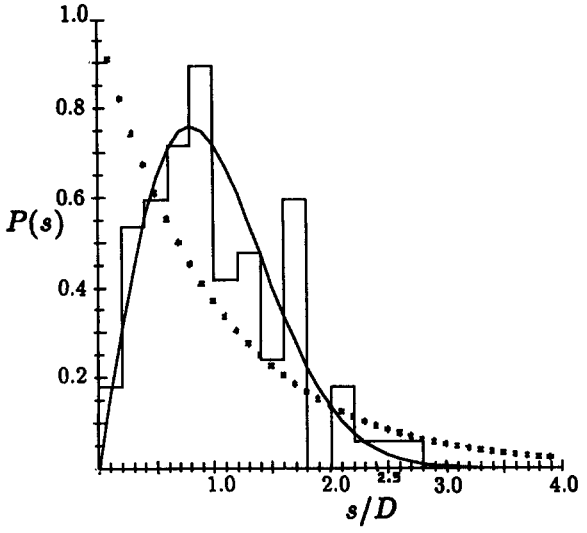

FIG. 2. The nearest-neighbor level spacings distribution for the A_2' representation. The first 84 levels are included, to about 187 cm^{-1}. Superimposed are the Poisson [Eq. (3), plotted with *] and Wigner [Eq. (4), plotted with solid line] distributions.

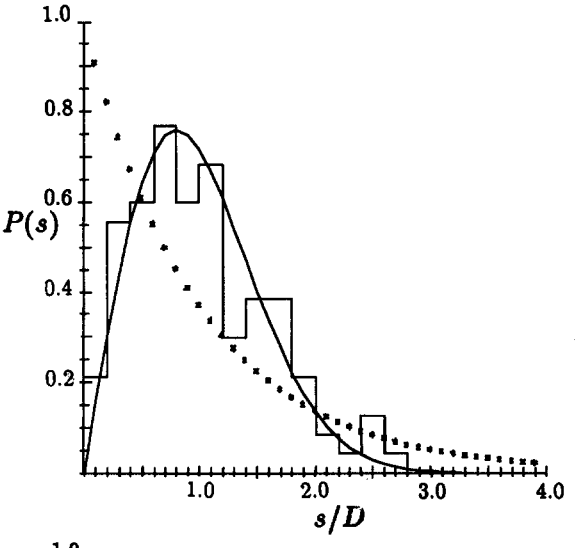

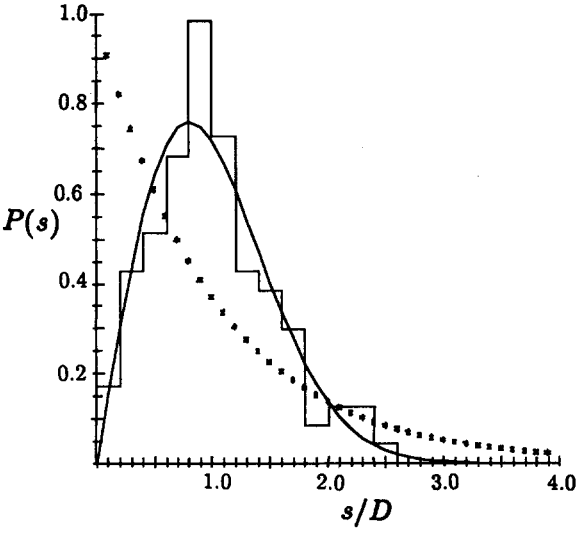

FIG. 3. The nearest-neighbor level spacings distribution for the E' representation. (a) the first 117 levels are included, to about 163 cm^{-1}. (b) includes the next 117 levels, to about 187 cm^{-1}. Superimposed are the Poisson [Eq. (3), plotted with *] and Wigner [Eq. (4), plotted with solid line] distributions.

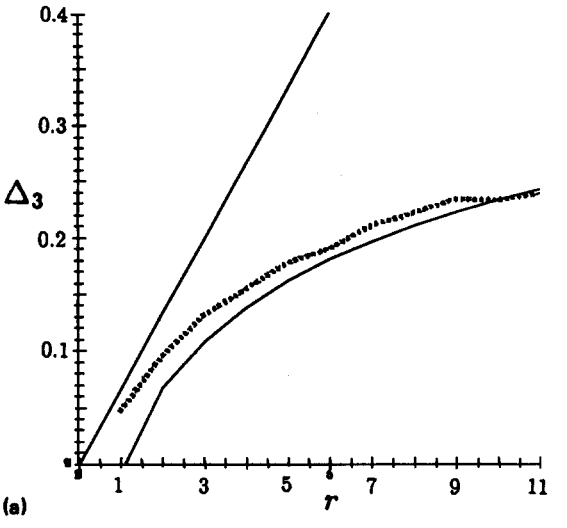

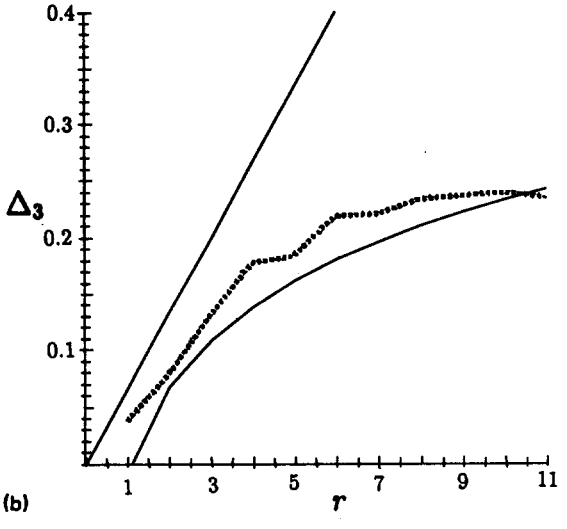

FIG. 4. The Δ_3 statistic for the A_1' representation. (a) is the first 66 levels, and (b) the next 66. Superimposed with solid lines are the GOE [Eq. (8)] and Poisson ($\Delta_3 = r/15$) relations.

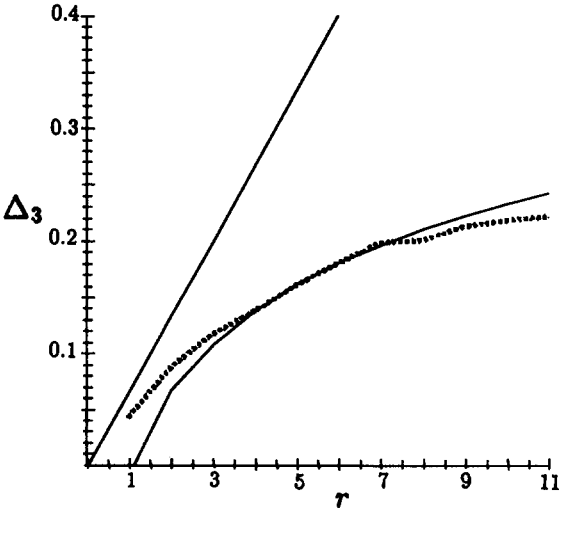

FIG. 5. The Δ_3 statistic for the A_2' representation. Superimposed with solid lines are the GOE [Eq. (8)] and Poisson ($\Delta_3 = r/15$) relations.

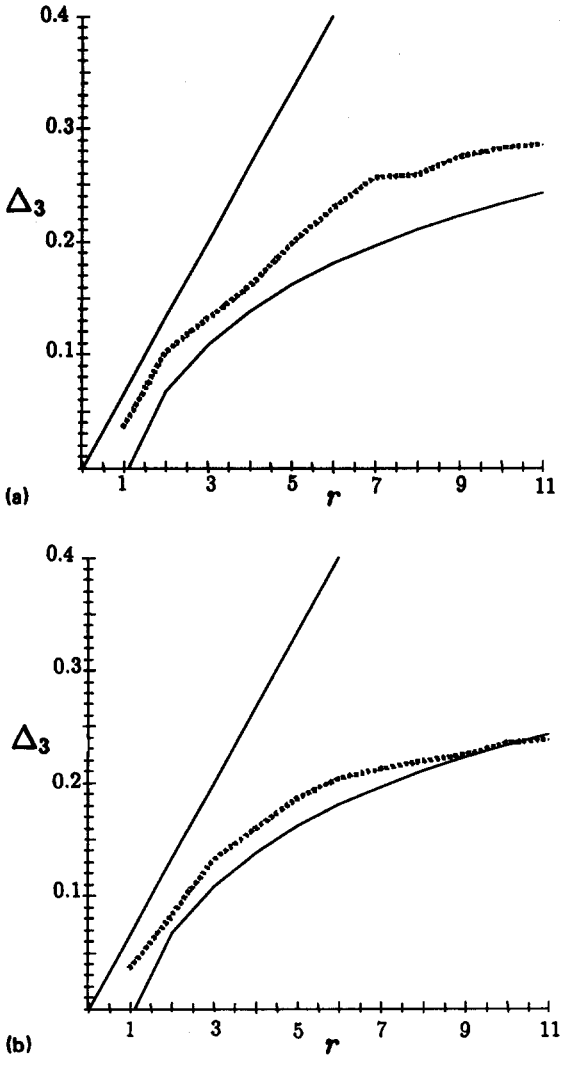

FIG. 6. The Δ_3 statistic for the E' representation. (a) is the first 117 levels, and (b) the next 117. Superimposed with solid lines are the GOE [Eq. (8)] and Poisson ($\Delta_3 = r/15$) relations.

GOE for each range, indicating no regular dynamics for any of the ranges considered. Unlike the classical study, where a transition to chaos was predicted, there is no such transition in the quantum system, since the ground state energy is higher than the energy at which the classical transition to chaos occurs.

With the advent of more powerful methods for calculating vibrational levels of molecules and van der Waals complexes, it has become possible to perform such statistical analyses of the eigenvalues. To date, few systems have been found to resemble GOE statistics. Statistics of the vibrational levels of molecules are often intermediate to Poisson and GOE, tending to GOE as the energy becomes greater. Most, therefore, have dynamics that are part regular and part unstable. Those that are fully chaotic are certainly ergodic, though we cannot say anything about the ergodicity for systems which are not fully chaotic.

ACKNOWLEDGMENTS

We thank Mario Feingold for many helpful discussions and a careful reading of the manuscript. The research presented here was supported by the National Science Foundation.

[1]T. L. Beck, D. M. Leitner, and R. S. Berry, J. Chem. Phys. **89**, 1681 (1988).
[2]D. M. Leitner, T. L. Beck, and R. S. Berry, J. Chem. Phys. (submitted).
[3]P. Butera and G. Caravati, Phys. Rev. A **36**, 2 (1987).
[4]Some extensive review articles are: M. V. Berry, in *Chaotic Behavior of Deterministic Systems, Les Houches, Session XXXVI* (North-Holland, Amsterdam, 1981); M. V. Berry, Proc. R. Soc. London Ser. A **413**, 183 (1987).
[5]E. Haller, H. Koppel, and L. S. Cederbaum, Chem. Phys. Lett. **101**, 3 (1983).
[6]G. Wunner, U. Woelk, I. Zech, G. Zeller, T. Ertl, F. Geyer, W. Schweizer, and H. Ruder, Phys. Rev. Lett. **57**, 3261 (1986).
[7]M. V. Berry and M. Robnik, J. Phys. A **17**, 2413 (1984).
[8]T. A. Brody, J. Flores, J. B. French, P. A. Mello, A. Pandey, and S. S. Wong, Rev. Mod. Phys. **53**, 385 (1981).
[9]Z. Bacic, R. M. Whitnell, D. Brown, and J. C. Light, Comp. Phys. Commun. **51**, 35 (1988); R. M. Whitnell and J. C. Light, J. Chem. Phys. **89**, 3674 (1988); **90**, 1774 (1989).
[10]M. V. Berry and M. Tabor, Proc. R. Soc. London Ser. A **356**, 375 (1979).
[11]F. J. Dyson and M. L. Mehta, J. Math. Phys. **4**, 701 (1963).
[12]M. Feingold and S. Fishman, Physica D **25**, 181 (1987).
[13]E. Abramson, R. W. Field, D. Imre, K. K. Innes, and J. L. Kinsey, J. Chem. Phys. **80**, 2298 (1984).